Title

Scavenger Receptor CD36 Directs Nonclassical Monocyte Patrolling Along the Endothelium During Early Atherogenesis

Journal

Arteriosclerosis Thrombosis and Vascular Biology, 37(11)

ISSN

1079-5642

Authors

Marcovecchio, Paola M
Thomas, Graham D
Mikulski, Zbigniew
et al.

Publication Date

2017-11-01

DOI

10.1161/atvbaha.117.309123

Peer reviewed

HHS Public Access

Author manuscript

Arterioscler Thromb Vasc Biol. Author manuscript; available in PMC 2018 November 01.

Published in final edited form as:

Arterioscler Thromb Vasc Biol. 2017 November ; 37(11): 2043–2052. doi:10.1161/ATVBAHA.117.309123.

Scavenger receptor CD36 directs nonclassical monocyte patrolling along the endothelium during early atherogenesis

Paola M. Marcovecchio[1,2], **Graham D. Thomas**[2], **Zbigniew Mikulski**[2], **Erik Ehinger**[2], **Karin A. L. Müller**[2,3], **Amy Blatchley**[2], **Runpei Wu**[2], **Yury I. Miller**[1], **Anh Tram Nguyen**[4], **Angela M. Taylor**[4], **Coleen A. McNamara**[4], **Klaus Ley**[2], and **Catherine C. Hedrick**[2,*]

[1]Department of Medicine, University of California San Diego School of Medicine La Jolla, California, USA

[2]Division of Inflammation Biology, La Jolla Institute for Allergy and Immunology, La Jolla, California, USA

[3]Department of Cardiology and Circulatory Diseases, Internal Medicine Clinic III, Eberhard Karls University Tübingen, Tübingen, Germany

[4]Robert M. Berne Cardiovascular Research Center, University of Virginia, Charlottesville, Virginia, USA

Abstract

Objective—Nonclassical monocytes function to maintain vascular homeostasis by crawling or patrolling along the vessel wall. This subset of monocytes responds to viruses, tumor cells, and other pathogens to aid in protection of the host. In this study, we wished to determine how early atherogenesis impacts nonclassical monocyte patrolling in the vasculature.

Approach and Results—To study the role of nonclassical monocytes in early atherogenesis, we quantified the patrolling behaviors of nonclassical monocytes in ApoE$^{-/-}$ and C57Bl/6J mice fed a Western diet. Using intravital imaging, we found that nonclassical monocytes from Western diet fed mice display a 4-fold increase in patrolling activity within large peripheral blood vessels. Both human and mouse nonclassical monocytes preferentially engulfed oxidized LDL in the vasculature, and we observed that oxidized LDL selectively induced nonclassical monocyte patrolling in vivo. Induction of patrolling during early atherogenesis required scavenger receptor CD36, as CD36$^{-/-}$ mice revealed a significant reduction in patrolling activity along the femoral vasculature. Mechanistically, we found that CD36-regulated patrolling was mediated by a Src family kinase (SFK) through DAP12 adaptor protein.

Conclusions—Our studies show a novel pathway for induction of nonclassical monocyte patrolling along the vascular wall during early atherogenesis. Mice fed a Western diet showed increased nonclassical monocyte patrolling activity with a concurrent increase in SFK phosphorylation. This patrolling activity was lost in the absence of either CD36 or Dap12. These

*Correspondence: Catherine C. Hedrick, PhD, Division of Inflammation Biology, La Jolla Institute for Allergy and Immunology, 9420 Athena Circle, La Jolla, CA 92037, Ph: 858-752-6500, hedrick@lji.org.

Disclosures

None.

data suggest that nonclassical monocytes function in an atheroprotective manner through sensing and responding to oxidized lipoprotein moieties via scavenger receptor engagement during early atherogenesis.

Introduction

Monocytes circulate in blood as predominantly 2 subsets: Ly6C^{+}CCR2^{high} and Ly6C^{-}CX$_3$CR1^{high} in mice, and CD14^{high}CD16^{dim} and CD14^{dim}CD16^{high} in humans, respectively[1]. Key experiments by several laboratories have shown that nonclassical Ly6C^{-}CX$_3$CR1^{high} monocytes (NCM) remain in circulation longer than classical Ly6C^{+}CCR2^{high} monocytes (CM), aid in vascular maintenance, and migrate to the sites of plaque formation during atherosclerosis[2–4]. Although other leukocytes can bind to and crawl along the endothelium, NCM appear to play the primary role of sentinels by patrolling the endothelium over long distances, often traveling against directional blood flow. A previous study by our group found that NCM are regulated by the transcription factor Nr4a1, and with the deletion of this gene, Ly6C^{-} monocytes are absent from blood and bone marrow[5]. *Nr4a1*$^{-/-}$ mice that were bred onto atherosclerosis-prone *Ldlr*$^{-/-}$ or *ApoE*$^{-/-}$ mice and fed a Western diet (WD) showed a 3-fold increase in atherosclerotic plaque formation and a greater inflammatory phenotype of macrophages in atherosclerotic lesions[6,7]. This study suggests that NCM likely play a role in the resolution of vessel inflammation during the onset of atherosclerosis. However, the effect of an atherogenic diet on vascular patrolling of NCM has not been examined in detail.

During atherogenesis, LDLs circulate in the bloodstream and eventually enter the subendothelial layer of the vessel wall, where they become trapped and oxidized to form modified forms of LDL[8]. These modified forms of LDL, such as minimally-modified LDL (mmLDL) and oxidized LDL (OxLDL), are considered immunogenic as well as atherogenic and can trigger leukocyte recruitment to the vascular wall[9,10]. Intimal cell proliferation and Ly6C^{+} monocyte recruitment to nascent lesions are markedly increased after 2 weeks of WD-feeding[11]. Scavenger receptors such as SR-A (class A), and CD36 (class B), recognize and bind to specific oxidized lipid moieties present on OxLDL[12, 13]. SR-A appears to signal in conjunction with Toll-like receptors (TLRs), as well as with Src family kinases (SFK) to mediate cell adhesion, possibly through G$_{i/o}$ signalling pathways[14–17]. On the other hand, CD36 can utilize DAP12 and/or FcRγ adaptor proteins to further signal to Syk and Src family kinases (SFK)[18,19]. As part of our goal to study NCM in early atherogenesis, we asked which key intracellular proteins are involved in the induction of NCM patrolling. The role of scavenger receptors and the intracellular signaling downstream of these receptors in NCM as they relate to patrolling has not been investigated.

Using a novel method of intravital imaging of the mouse femoral vasculature during atherogenesis, we show that NCM preferentially internalize OxLDL through a scavenger receptor-mediated process involving DAP12 and SFK that induces their patrolling along the endothelium.

Materials and Methods

Materials and Methods are available in the online-only Data Supplement.

Results

Increased Ly6C^{-} nonclassical monocyte patrolling along large peripheral blood vessel endothelium during early atherogenesis

We hypothesized that vascular inflammation during atherogenesis in large blood vessels would lead to changes in nonclassical monocyte (NCM) patrolling activity. In order to address this, we used an established a mouse model of early atherosclerosis by feeding a high fat Western diet (0.2% cholesterol, 42% calories from fat) to ApoE$^{-/-}$ mice or C57BL/6J (B6) mice for up to 28 days[20–23]. Age and sex-matched groups of B6 or ApoE$^{-/-}$ mice crossed to $CX_3CR1^{gfp/+}CCR2^{rfp/+}$ reporter mice were fed a WD for either 1 day or 28 days and imaged for patrolling activity of $CX_3CR1^{high}CCR2^{low}$ monocytes using a novel femoral artery imaging method (described in Supplemental Figure I). These mice enable us to visualize both NCM ($CX_3CR1^{gfp/+}$) and classical monocytes (CM) ($CCR2^{rfp/+}$) by confocal microscopy as expression of CX_3CR1 is higher on NCM and expression of CCR2 is higher on CM[1]. NCM from WD-fed mice showed a significant 4-fold increase in patrolling activity along the vascular endothelium in vivo compared to NCM from chow-fed mice (Figure 1, A and B). This increase was observed even after one day of WD-feeding and is sustained through 4 weeks of WD-feeding. When either B6 or ApoE$^{-/-}$ mice were placed on WD for 2 weeks and subsequently put back on chow for an equal amount of time, the NCM showed reduced patrolling activity, almost reverting to the levels of pre-WD-feeding (Figure 1A, Regression). The overall speed monocyte patrolling was also affected by WD-feeding (Figure 1C), as chow-fed mice exhibited the expected average of 12 μm/minute (ranging from 6-24 μm/minute)[24], but NCM from WD-fed mice had reduced patrolling speeds, down to 5 μm/minute (ranging from 2-10 μm/minute). Additional characteristics such as track length, track displacement (distance from start point to end point of track), and confinement (displacement/length, 0 = circular track, 1 = straight track), were not significantly different (Supplemental Figure IIA).

Earlier studies have reported that ApoE$^{-/-}$ mice fed a WD develop monocytosis in the Ly6C^{+} compartment[4,25,26]. We wanted to confirm that the observed increase in patrolling activity was not due simply to increased numbers of NCM present in the blood during atherogenesis. We measured the frequency of Ly6C^{-} monocytes in chow-fed mice and WD-fed mice by flow cytometry. In both B6 and ApoE$^{-/-}$ mice, we observed an increase in the frequency of classical Ly6C^{+} monocytes (Supplemental Figure IIB), but not Ly6C^{-} monocytes (Figure 1D). Additionally, we measured monocyte proliferation using BrdU incorporation. We found that Ly6C^{+} monocytes incorporated BrdU in 50-70% of cells by 48 hours in WD-fed mice compared to only 0.5-1% incorporation into Ly6C^{-} monocytes (Supplemental Figure IIC). Importantly, these data indicate that during early atherogenesis, the increase in patrolling of Ly6C^{-} monocytes on blood vessel walls is due to changes in activation of NCM and not the result of increased numbers of NCM circulating in the blood.

Sequencing analysis of nonclassical monocytes in early atherogenesis shows increased expression of genes involved in cell migration, cholesterol efflux, and vascular repair

To determine if there were gene expression changes in monocyte subsets during atherogenesis that were related to functional changes in patrolling activity, we sorted CM and NCM from 8 week WD-fed mice and cohort chow-fed mice (gating strategy shown in Supplemental Figure IIIA) and performed RNA-seq analysis. Genes that are involved in cell migration (Rab GTPase activation, kinases, integrin activation, and lamellipodia components)[27–29] and resolution of inflammation/vascular repair were more highly expressed in Ly6C$^-$ monocytes from WD-fed mice than in Ly6C$^-$ monocytes fed chow or in Ly6C$^+$ monocytes (Figure 2A)[30].

Based on our earlier studies using global *Nr4a1*$^{-/-}$ mice[6], we hypothesized that an absence of patrolling by Ly6C$^-$ monocytes would increase atherosclerotic progression. We generated mice selectively lacking Ly6C$^-$ monocytes (E2-def) with no observable changes in any other immune cell type in vivo[31], and transplanted bone marrow from either WT or E2-def mice into *Ldlr*$^{-/-}$ recipients. After checking for successful bone marrow reconstitution (Supplemental Figure IIIB) and feeding a high cholesterol diet for 15 weeks, we assessed plaque formation by Oil Red O staining in WT-Ldlr$^{-/-}$ and E2-def-Ldlr$^{-/-}$ mice. We found a 2-fold increase in plaque formation in E2-deficient mice selectively lacking NCM (Figure 2B and 2C), indicating that nonclassical monocytes are functionally atheroprotective.

We next examined whether NCM showed differences in free or esterified cholesterol accumulation. Blood monocytes from mice and humans (gating strategies shown in Supplemental Figure IIIA and C, respectively) were stained with either Bodipy (identifies esterified cholesterol/lipid droplets) or filipin (identifies free cholesterol). Mouse NCM had lower cholesteryl ester content (Figure 2D) than CM, even after 4 weeks of WD feeding. We observed no changes in filipin staining (Figure 2E). Human nonclassical CD16$^+$ monocytes also had lower cholesteryl ester content than CD14$^+$ classical monocytes (Figure 2F). This correlates with our RNA-seq findings of increased mRNA expression of both of the key cholesterol transporters, ABCG1 and ABCA1, in NCM isolated from WD-fed mice (Figure 2A), suggesting that these transporters regulate the cholesterol content of NCM.

F-actin formation is increased in NCM from WD-fed mice

Leukocyte migration involves high-affinity conformation integrin activation, allowing the cell to bind to endothelial cell surface ligands and form lamellipodia for patrolling, which involves the polymerization and depolymerization of filamentous-actin (F-actin) in a front-to-rear wave-like pattern. Many of the genes that were specifically upregulated in Ly6C$^-$ monocytes from WD-fed mice are involved in either integrin activation or in forming cellular cytoskeletal structures necessary for cell crawling along the vasculature. Initially we asked whether Gαi chemokine receptors were involved in inducing patrolling during atherogenesis. We measured patrolling NCM in WD-fed mice before and after pertussis toxin injections and could not find a significant decrease in patrolling frequency or any change in patrolling speeds (Supplemental Figure IVA). We then measured integrin expression in both monocytes from WD-fed mice (Supplemental Figure IVB,C) as well as

from human subjects with documented CAD (Supplemental Figure IVD), but found no significant changes.

We next measured F-actin formation in blood monocyte subsets from chow-fed or WD-fed mice by confocal microscopy using phalloidin-AF488, a phallotoxin that binds to and stabilizes filamentous actin. Monocytes sorted from WD-fed mice exhibited greater F-actin content than monocytes from chow-fed mice (Figure 3A). When F-actin intensity was quantified for each cell within each condition, the $Ly6C^{-}$ monocytes from WD-fed mice had increased F-actin content compared to the $Ly6C^{+}$ subset (Figure 3B). These data suggest that $Ly6C^{-}$ NCM more readily form the machinery necessary for cell motility within blood vessels, particularly in WD-fed mice.

Oxidized lipoprotein moieties present in early atherogenesis induce NCM patrolling

Previous studies have reported that human and mouse NCM do not ingest native LDL (LDL) or very low-density lipoproteins (VLDL) as much as do CM[32], so we tested whether blood NCM would preferentially uptake modified forms of LDL. $CX_3CR1^{gfp/+}CCR2^{rfp/+}ApoE^{-/-}$ mice were injected intravenously with fluorescently-labeled LDL, native LDL protected from oxidation by BHT (BHT-LDL), minimally modified LDL (mmLDL)[33,34] and copper-oxidized LDL (OxLDL). Flow cytometry analysis showed that OxLDL was preferentially taken up by NCM in the circulation (Figure 4A). Compared to CM, NCM showed 2-fold increased uptake of OxLDL (Figure 4B). We next looked at F-actin formation by confocal microscopy in NCM when OxLDL was added (Figure 4C). Again we saw a significant increase in F-actin intensity in the presence of OxLDL (Figure 4D), suggesting that OxLDL can mobilize NCM to adhere to the endothelium and patrol.

To determine whether OxLDL could directly increase patrolling monocyte activity, either OxLDL, nLDL, or vehicle (PBS) was injected intravenously into $CX_3CR1^{gfp/+}CCR2^{rfp/+}ApoE^{-/-}$ mice (Figure 4E). Patrolling monocytes were quantified pre- and post-injection by imaging an area of the femoral vasculature over time. We found that OxLDL injection significantly induced CX_3CR1^{high} nonclassical monocyte patrolling along the endothelium (Figure 4E, lower panels), while PBS (Figure 4E, upper panel) and LDL (data not shown) did not.

We next characterized the patrolling behavior of NCM that had ingested OxLDL. Within 10 minutes post-injection, CX_3CR1^{high} NCM had taken up DiI-OxLDL, which localized to the rear cell body and not in the leading edge of the lamellipodia (Figure 4F and Supplemental Video 1). At no point did we observe extravasation of the monocytes into the surrounding leg muscle tissue in mice fed either chow or WD. However, we did notice a “slingshot” behavior of CX_3CR1^{high} nonclassical monocytes that rapidly attached to the endothelium and immediately transitioned into patrolling (Supplemental Video 2). These results suggest that oxidized lipoprotein moieties present in the vasculature during early atherogenesis bind to scavenger receptors on NCM and induce an activation cascade that triggers nonclassical monocyte patrolling.

Nonclassical monocytes lacking CD36 fail to patrol the vasculature in early atherogenesis

CD36 and Msr1 (SR-A) are known scavenger receptors involved in the uptake of oxidized LDL[10]. Based on our data that illustrate that NCM preferentially uptake OxLDL and that this OxLDL uptake changes the F-actin content of NCM (Figure 3), we examined monocyte patrolling in mice lacking either the class A scavenger receptor, Msr1 or the class B scavenger receptor CD36, or both. *Msr1*$^{-/-}$, *CD36*$^{-/-}$, or *Msr1*$^{-/-}$*CD36*$^{-/-}$ double knockout (DKO) mice were fed a WD for 28 days prior to imaging. Circulating NCM in these mice were labeled with CD115-AF488 and FcγRIV(CD16.2)-PE[35] for imaging. We found that monocytes from WD-fed *CD36*$^{-/-}$ or DKO mice showed significantly reduced patrolling in response to WD, and in some of the *CD36*$^{-/-}$ or DKO mice, patrolling was completely abolished (Figure 5A). Fewer *CD36*$^{-/-}$ NCM patrolled the endothelium (Figure 5B), although the numbers of NCM present in blood were similar in WT vs *CD36*$^{-/-}$ mice (Figure 5C). Of the NCM that did patrol in the *CD36*$^{-/-}$ and *Msr1*$^{-/-}$ or DKO mice, mean speeds of patrolling were significantly reduced (Figure 5D). Interestingly, the patrolling characteristics of the NCM were different in the *Msr1*$^{-/-}$ mice (Supplemental Figure VA), such that they uniformly patrolled slower and straighter over shorter distances relative to WT or *CD36*$^{-/-}$ mice, suggesting loss of directional control in absence of OxLDL sensing. NCM from mice transplanted with DKO bone marrow predominantly exhibited patrolling characteristics very similar to that of the global *CD36*$^{-/-}$ model (Figure 5A,D and Supplemental Figure VA,B). *CD36*$^{-/-}$ NCM showed significantly reduced uptake of OxLDL (Figure 5E). We also observed a slight reduction in OxLDL uptake of *Msr1*$^{-/-}$ mice, but not to the significant extent of *CD36*$^{-/-}$ mice (Supplemental Figure VC).

To determine if CD36 expression on the NCM rather than on vascular endothelium was critical in directing patrolling behavior, we performed a BMT where we transplanted WT bone marrow into either WT or *CD36*$^{-/-}$ recipients. We found that patrolling behavior was similar in WT and *CD36*$^{-/-}$ recipients, confirming that deletion of *CD36*$^{-/-}$ on the endothelium plays an insignificant role in directing NCM patrolling (Figure 5F and Supplemental Figure VD). Additionally, we tested NCM from *TLR7*$^{-/-}$ or *CX*$_3$*CR1*$^{-/-}$ mice for patrolling activity based on our previous reports that illustrated that these receptors played functional roles in NCM[3,36]. Neither receptor played a role in orchestrating the patrolling behavior of NCM in response to WD feeding (Supplemental Figure VE).

Human CD16^{+} nonclassical monocytes also possess scavenger receptors capable of binding and internalizing OxLDL, including CD163 (scavenger receptor class I), SR-A (CD204), and to a lesser extent CD36 (Supplemental Figure VIA). They also possess high levels of tetraspanin CD81 (Supplemental Figure VIA), which has been shown to associate with CD36 and assists in internalizing the receptor upon binding to OxLDL[18]. Although expression is much higher in mouse NCM, transcript and protein levels of CD36 in human NCM are detectable by qPCR (Supplemental Figure VIB) and flow cytometry (Figure 5G). Moreover, when whole blood from healthy donors was incubated with various forms of LDL, similar to the in vivo injections in mouse, OxLDL was preferentially taken up by CD16^{+} monocytes (Figure 5H).

Ly6C^{-} monocytes utilize Src family kinases and DAP12 to patrol during early atherosclerosis

CD36 lacks a cytoplasmic tail that can propagate signalling cascades on its own and must rely on adapter proteins[18]. We examined the effect of deleting DAP12, a known CD36-associated adapter protein, on NCM patrolling in WD-fed mice. We transplanted DAP12$^{-/-}$ bone marrow into WT recipients, let mice recover and then fed the mice WD for 28 days. After WD feeding, we observed a significant 2-fold reduction in the number of NCM patrolling the vasculature (Figure 6A). Moreover, the mean speed of NCM patrolling along the vasculature was higher in the absence of DAP12 (Figure 6B), suggesting that the NCM lacking DAP12 could not adequately respond to the presence of OxLDL in vivo. There was no significant difference in the frequency of NCM in blood of DAP12$^{-/-}$ mice (Supplemental Figure VIIA).

Next, we examined which kinases might be acting downstream of CD36. We inhibited phosphorylation of Syk and SFK, two kinases known to transduce signals between receptors and integrins, We injected either PP1, a reversible cell permeable SFK inhibitor, or Piceatannol, a cell permeable Syk phosphorylation inhibitor, intravenously into WD-fed $CX_3CR1^{gfp/+}CCR2^{rfp/+}ApoE^{-/-}$ mice and imaged NCM patrolling (Figure 6C). Within 20 minutes of injection, NCM that had been actively patrolling either arrested or detached from the endothelium (Figure 6C). When vehicle (equal amount DMSO diluted with PBS) was injected by the same route, patrolling monocytes continued to crawl along the vasculature undisturbed (Figure 6C). In contrast, injection of Piceatannol had no effect on patrolling (Figure 6C and Supplemental Figure VIIB).

We next performed immunoblotting for active-site phosphorylation of SFKs in NCM from chow or WD-fed WT or *CD36*$^{-/-}$ mice or from WT WD-fed mice treated with PP1. We used the pan-pSFK Y416 antibody, which recognizes SFK phosphorylation at the Y416 active site. NCM from WD-fed mice showed activation of SFKs as measured by Y416 phosphorylation (Figure 6D). Phosphorylation was abrogated with addition of the PP1 inhibitor (Figure 6D). Importantly, NCM from *CD36*$^{-/-}$ mice showed no activated pSFK (Figure 6D), supporting the notion that ligand binding of CD36 requires downstream activation of SFKs to induce patrolling. Thus, NCM require CD36-ligand binding and signalling through DAP12 to activate SFKs for inducing patrolling along blood vessel walls in WD-fed mice.

Discussion

In this study, we examine how NCM patrolling behavior is changed in early atherogenesis. We found that patrolling by NCM is significantly increased in the vasculature during early atherogenesis, and that patrolling in this setting was triggered by scavenger receptor recognition and uptake of oxidized LDL, primarily through CD36, and to a lesser extent, SR-A. This signal is transmitted through DAP12 and SFKs, culminating in changes in F-actin formation in NCM, leading to patrolling along the vascular endothelium. Our data suggest that SFK and DAP12 are working downstream of CD36 to promote integrin activation and dynamic changes in F-actin that lead to patrolling.

We also examined patrolling activity of NCM in *Msr1*$^{-/-}$ mice. We did not observe a significant difference in patrolling frequency in the global *Msr1*$^{-/-}$ mice, nor did we detect a significant change in OxLDL uptake by *Msr1*$^{-/-}$ NCM. It is possible that changes in the patrolling characteristics of NCM in *Msr1*$^{-/-}$ mice may be contributed by the endothelium. In the *Msr1*$^{-/-}$*CD36*$^{-/-}$ double knockout bone marrow transfer experiment that we performed, CD36 behaved as the dominant receptor on NCM, as the patrolling frequency and characteristics of these monocytes looked similar to *CD36*$^{-/-}$ mice. We further examined *CD36*$^{-/-}$ recipient mice that had been transplanted with WT bone marrow to explore how selective endothelial loss of CD36 would impact patrolling. We found no changes in patrolling behavior in the absence of endothelial CD36, suggesting that endothelial CD36 had little impact on regulation of NCM patrolling in WD-fed mice. Further, we examined the role of DAP12, a CD36-adaptor protein, and found that absence of DAP12 in NCM significantly reduced, but did not completely abolish, patrolling. Thus, other pathways, in addition to CD36, likely play a role in regulating NCM patrolling in response to WD-feeding during early atherogenesis.

Previous studies[24,37] have shown that LFA-1 and VLA-4 integrins mediate patrolling, particularly in atherosclerotic mice. It has been proposed that $G_{\alpha i}$ chemokine receptors are necessary for inducing patrolling in NCM during inflammation[36]. However, we did not observe significant reductions in NCM patrolling after pertussis toxin injections of WD-fed mice. We propose that integrin changes in affinity conformation are responsible for the increase in patrolling, and that this is due to CD36 activation in response to OxLDL sensing in early atherogenesis. Due to the lack of integrin conformation-specific antibodies available for mice, and because the human CAD patient samples used in our study were processed using EDTA (which prevents integrins from reaching high-affinity conformations), we could not directly link CD36 with integrin conformational changes. However, we have shown that F-actin formation, which is necessary for cell motility, is indeed increased in NCM from WD-fed mice, as well as when OxLDL is bound to NCM.

As a scavenger receptor, CD36 can bind to multiple ligands, including OxLDL and apoptotic cells via recognition of oxidized phosphatidylserine and oxidized phospholipids[38]. Studies from our laboratory and others have shown than NCM scavenge apoptotic endothelial cells, and tumor debris in the vasculature[36]. Further, NCM can migrate to and enter sites of atherosclerotic plaque formation in mice[4]. Whether the trigger for NCM patrolling in early atherogenesis is OxLDL itself or some oxidized moiety present in the OxLDL that is a ligand for scavenger receptors is unclear. Thus, we cannot rule out that other ligands or other oxidized LDL moieties are binding to CD36 on NCM during atherosclerosis and triggering patrolling. It is clear that the absence of NCM increases plaque formation in mice, but the exact roles of CD36 on NCM as it pertains to atherosclerosis progression remains a question for future studies.

SFKs consist of several members shown to be involved in signal transduction that are present in monocytes including Src, Lyn, and Fyn. We found that NCM from WD-fed mice have higher levels of phosphorylated SFK at the activation site Y416 using a pan-SFK antibody. Further, in vivo administration of the SFK inhibitor PP1 abrogated patrolling. In support of this, we have observed that Csk, a negative regulator of SFK, is increased in

NCM in WD-fed mice (Figure 2A), further suggesting that SFKs are activated in NCM during WD-feeding[39]. Conversely, in vivo administration of Piceatannol (Syk inhibitor) failed to abolish patrolling in WD-fed mice, suggesting that Syk is not involved in regulation of CD36-mediated NCM patrolling in atherogenesis. We have not yet definitively determined which SFK contributes to CD36-mediated NCM patrolling.

In contrast to mouse monocytes, human $CD14^{dim}CD16^{+}$ monocytes have low levels of CD36 expression compared to the classical subset. However, human $CD14^{dim}CD16^{+}$ monocytes do express some low levels of CD36 and higher levels of the CD36-associated tetraspanin CD81. In addition, they possess relatively abundant levels of other scavenger receptors that are capable of taking up OxLDL, such as SR-A and CD163. We found that OxLDL is indeed preferentially taken up by human NCM, which may be bound by CD36 or one of the other more abundant scavenger receptors that can bind OxLDL.

In summary, by using intravital imaging in vivo to examine nonclassical monocyte function in large peripheral blood vessels during early stages of atherosclerosis, we have discovered that nonclassical monocytes respond to oxidized LDL and show increased patrolling along the vascular endothelium. In mice, this appears to be mediated by CD36, and recognition of OxLDL by CD36 causes downstream activation of Src family kinases, which promote cytoskeletal changes, leading to increased patrolling. Further studies to dissect the role of CD36 in nonclassical monocyte activation during atherogenesis will enhance our understanding of how the innate immune system controls inflammation and atherosclerotic plaque formation.

Supplementary Material

Refer to Web version on PubMed Central for supplementary material.

Acknowledgments

We would like to thank Deborah Yoakum for all mouse breeding and the LJI Flow Cytometry core assistance with cell sorting. We would like to thank the LJI Microscopy Core, particularly Zbigniew Mikulski, Sara McArdle, and William Kiosses for helpful discussions. We would also like to thank Dr Jessica Hamerman, Benaroya Institute for the kind gift of the $DAP12^{-/-}$ bone marrow and Dr Dr. Ronit Shiri-Sverdlov, Maastricht University, Netherlands for the kind gift of the $Msr1^{-/-}CD36^{-/-}$ bone marrow. We would like to thank Dr Maria Febbraio, University of Alberta, CA for helping us obtain $Msr1^{-/-}CD36^{-/-}$ marrow.

Sources of funding

This work was supported by NIH F31 HL132538 (to PMM), NIH R01 HL134236 and HL118765 (both to CCH), P01 HL055798 (to CCH, CAM, AMT, KL, and YM), and AHA Fellowship 16POST27630002 (to GDT).

Abbreviations

ApoE	apolipoprotein E
BHT	butylated hydroxytoluene
BrdU	bromodeoxyuridine
CAD	coronary artery disease

CM	classical monocytes
DAP12	DNAX Activating Protein of 12KDa
FACS	fluorescence-activated cell sorting
gMFI	geometric mean fluorescence intensity
ICAM	intercellular adhesion molecule
mmLDL	minimally modified low-density lipoprotein
Msr1	macrophage scavenger receptor 1
nLDL	native low-density lipoprotein
NCM	nonclassical monocytes
OxLDL	oxidized low-density lipoprotein
RBC	red blood cell
SFK	src family kinase
SR-A	scavenger receptor-class A
Syk	spleen tyrosine kinase
TLR	toll-like receptor
VCAM	vascular cell adhesion molecule
VLDL	very low-density lipoprotein
WD	western diet
WT	wild-type

References

1. Geissmann F, Jung S, Littman DR. Blood monocytes consist of two principal subsets with distinct migratory properties. Immunity. 2003; 19:71–82. [PubMed: 12871640]
2. Yona S, Kim K-W, Wolf Y, Mildner A, Varol D, Breker M, Strauss-Ayali D, Viukov S, Guilliams M, Misharin A, Hume DA, Perlman H, Malissen B, Zelzer E, Jung S. Fate mapping reveals origins and dynamics of monocytes and tissue macrophages under homeostasis. Immunity. 2013; 38:79–91. [PubMed: 23273845]
3. Auffray C, Fogg D, Garfa M, Elain G, Join-Lambert O, Kayal S, Sarnacki S, Cumano A, Lauvau G, Geissmann F. Monitoring of blood vessels and tissues by a population of monocytes with patrolling behavior. Science. 2007; 317:666–670. [PubMed: 17673663]
4. Tacke F, Alvarez D, Kaplan TJ, Jakubzick C, Spanbroek R, Llodra J, Garin A, Liu J, Mack M, van Rooijen N, Lira SA, Habenicht AJ, Randolph GJ. Monocyte subsets differentially employ CCR2, CCR5, and CX3CR1 to accumulate within atherosclerotic plaques. J Clin Invest. 2007; 117:185–194. [PubMed: 17200718]
5. Hanna RN, Carlin LM, Hubbeling HG, Nackiewicz D, Green AM, Punt JA, Geissmann F, Hedrick CC. The transcription factor NR4A1 (Nur77) controls bone marrow differentiation and the survival of Ly6C- monocytes. Nat Immunol. 2011; 12:778–785. [PubMed: 21725321]

6. Hanna RN, Shaked I, Hubbeling HG, Punt JA, Wu R, Herrley E, Zaugg C, Pei H, Geissmann F, Ley K, Hedrick CC. NR4A1 (Nur77) deletion polarizes macrophages toward an inflammatory phenotype and increases atherosclerosis. Circ Res. 2012; 110:416–427. [PubMed: 22194622]
7. Hamers AAJ, Vos M, Rassam F, Marinković G, Marincovic G, Kurakula K, van Gorp PJ, de Winther MPJ, Gijbels MJJ, de Waard V, de Vries CJM. Bone marrow-specific deficiency of nuclear receptor Nur77 enhances atherosclerosis. Circ Res. 2012; 110:428–438. [PubMed: 22194623]
8. Tabas I, Ira T, Guillermo G-C, Owens GK. Recent insights into the cellular biology of atherosclerosis. J Cell Biol. 2015; 209:13–22. [PubMed: 25869663]
9. Tsimikas S, Miller YI. Oxidative Modification of Lipoproteins: Mechanisms, Role in Inflammation and Potential Clinical Applications in Cardiovascular Disease. Curr Pharm Des. 2011; 17:27–37. [PubMed: 21226665]
10. Miller YI, Choi S-H, Wiesner P, Fang L, Harkewicz R, Hartvigsen K, Boullier A, Gonen A, Diehl CJ, Que X, Montano E, Shaw PX, Tsimikas S, Binder CJ, Witztum JL. Oxidation-specific epitopes are danger-associated molecular patterns recognized by pattern recognition receptors of innate immunity. Circ Res. 2011; 108:235–248. [PubMed: 21252151]
11. Zhu S-N, Chen M, Jongstra-Bilen J, Cybulsky MI. GM-CSF regulates intimal cell proliferation in nascent atherosclerotic lesions. J Exp Med. 2009; 206:2141–2149. [PubMed: 19752185]
12. Febbraio M, Abumrad NA, Hajjar DP, Sharma K, Cheng W, Pearce SF, Silverstein RL. A null mutation in murine CD36 reveals an important role in fatty acid and lipoprotein metabolism. J Biol Chem. 1999; 274:19055–19062. [PubMed: 10383407]
13. Nicholson AC, Frieda S, Pearce A, Silverstein RL. Oxidized LDL binds to CD36 on human monocyte-derived macrophages and transfected cell lines. Evidence implicating the lipid moiety of the lipoprotein as the binding site. Arterioscler Thromb Vasc Biol. 1995; 15:269–275. [PubMed: 7538425]
14. Post SR. Class A scavenger receptors mediate cell adhesion via activation of Gi/o and formation of focal adhesion complexes. J Lipid Res. 2002; 43:1829–1836. [PubMed: 12401881]
15. Nikolic DM, Cholewa J, Gass C, Gong MC, Post SR. Class A scavenger receptor-mediated cell adhesion requires the sequential activation of Lyn and PI3-kinase. AJP: Cell Physiology. 2006; 292:C1450–C1458. [PubMed: 17192284]
16. Yu H, Ha T, Liu L, Wang X, Gao M, Kelley J, Kao R, Williams D, Li C. Scavenger receptor A (SR-A) is required for LPS-induced TLR4 mediated NF-κB activation in macrophages. Biochim Biophys Acta. 2012:18231192–1198.
17. Miki S, Tsukada S, Nakamura Y, Aimoto S, Hojo H, Sato B, Yamamoto M, Miki Y. Functional and possible physical association of scavenger receptor with cytoplasmic tyrosine kinase Lyn in monocytic THP-1-derived macrophages. FEBS Lett. 1996; 399:241–244. [PubMed: 8985154]
18. Heit B, Kim H, Cosío G, Castaño D, Collins R, Lowell CA, Kain KC, Trimble WS, Grinstein S. Multimolecular signaling complexes enable Syk-mediated signaling of CD36 internalization. Dev Cell. 2013; 24:372–383. [PubMed: 23395392]
19. Stuart LM, Bell SA, Stewart CR, Silver JM, Richard J, Goss JL, Tseng AA, Zhang A, El Khoury JB, Moore KJ. CD36 signals to the actin cytoskeleton and regulates microglial migration via a p130Cas complex. J Biol Chem. 2007; 282:27392–27401. [PubMed: 17623670]
20. Jongstra-Bilen J, Haidari M, Zhu S-N, Chen M, Guha D, Cybulsky MI. Low-grade chronic inflammation in regions of the normal mouse arterial intima predisposed to atherosclerosis. J Exp Med. 2006; 203:2073–2083. [PubMed: 16894012]
21. Paigen B, Morrow A, Holmes PA, Mitchell D, Williams RA. Quantitative assessment of atherosclerotic lesions in mice. Atherosclerosis. 1987; 68:231–240. [PubMed: 3426656]
22. Zhang SH, Reddick RL, Piedrahita JA, Maeda N. Spontaneous hypercholesterolemia and arterial lesions in mice lacking apolipoprotein E. Science. 1992; 258:468–471. [PubMed: 1411543]
23. Plump AS, Smith JD, Hayek T, Aalto-Setälä K, Walsh A, Verstuyft JG, Rubin EM, Breslow JL. Severe hypercholesterolemia and atherosclerosis in apolipoprotein E-deficient mice created by homologous recombination in ES cells. Cell. 1992; 71:343–353. [PubMed: 1423598]
24. Auffray C, Fogg D, Garfa M, Elain G, Join-Lambert O, Kayal S, Sarnacki S, Cumano A, Lauvau G, Geissmann F. Monitoring of blood vessels and tissues by a population of monocytes with patrolling behavior. Science. 2007; 317:666–670. [PubMed: 17673663]

25. Murphy AJ, Akhtari M, Tolani S, Pagler T, Bijl N, Kuo C-L, Wang M, Sanson M, Abramowicz S, Welch C, Bochem AE, Kuivenhoven JA, Yvan-Charvet L, Tall AR. ApoE regulates hematopoietic stem cell proliferation, monocytosis, and monocyte accumulation in atherosclerotic lesions in mice. J Clin Invest. 2011; 121:4138–4149. [PubMed: 21968112]
26. Swirski FK, Libby P, Aikawa E, Alcaide P, Luscinskas FW, Weissleder R, Pittet MJ. Ly-6Chi monocytes dominate hypercholesterolemia-associated monocytosis and give rise to macrophages in atheromata. J Clin Invest. 2007; 117:195–205. [PubMed: 17200719]
27. Stenmark H. Rab GTPases as coordinators of vesicle traffic. Nat Rev Mol Cell Biol. 2009; 10:513–525. [PubMed: 19603039]
28. Rottner K, Behrendt B, Small JV, Wehland J. VASP dynamics during lamellipodia protrusion. Nat Cell Biol. 1999; 1:321–322. [PubMed: 10559946]
29. Moser M, Nieswandt B, Ussar S, Pozgajova M, Fässler R. Kindlin-3 is essential for integrin activation and platelet aggregation. Nat Med. 2008; 14:325–330. [PubMed: 18278053]
30. Michelucci A, Cordes T, Ghelfi J, Pailot A, Reiling N, Goldmann O, Binz T, Wegner A, Tallam A, Rausell A, Buttini M, Linster CL, Medina E, Balling R, Hiller K. Immune-responsive gene 1 protein links metabolism to immunity by catalyzing itaconic acid production. Proc Natl Acad Sci U S A. 2013; 110:7820–7825. [PubMed: 23610393]
31. Thomas GD, Hanna RN, Vasudevan NT, Hamers AA, Romanoski CE, McArdle S, Ross KD, Blatchley A, Yoakum D, Hamilton BA, Mikulski Z, Jain MK, Glass CK, Hedrick CC. Deleting an Nr4a1 Super-Enhancer Subdomain Ablates Ly6C(low) Monocytes while Preserving Macrophage Gene Function. Immunity. 2016; 45:975–987. [PubMed: 27814941]
32. Jackson WD, Weinrich TW, Woollard KJ. Very-low and low-density lipoproteins induce neutral lipid accumulation and impair migration in monocyte subsets. Sci Rep. 2016; 6:20038. [PubMed: 26821597]
33. Liao F, Berliner JA, Mehrabian M, Navab M, Demer LL, Lusis AJ, Fogelman AM. Minimally modified low density lipoprotein is biologically active in vivo in mice. J Clin Invest. 1991; 87:2253–2257. [PubMed: 2040705]
34. Steinbrecher UP, Parthasarathy S, Leake DS, Witztum JL, Steinberg D. Modification of low density lipoprotein by endothelial cells involves lipid peroxidation and degradation of low density lipoprotein phospholipids. Proc Natl Acad Sci U S A. 1984; 81:3883–3887. [PubMed: 6587396]
35. Ingersoll, Molly A., Spanbroek, Rainer, Lottaz, Claudio, Gautier, Emmanuel L., Frankenberger, Marion, Hoffmann, Reinhard, Rol, Lang, Haniffa, Muzlifah, Collin, Matthew, Tacke, Frank, Habenicht, Andreas JR., Ziegler-Heitbrock, Loems, Randolph, Gwendalyn J. Comparison of gene expression profiles between human and mouse monocyte subsets. Blood. 2010; 115:e10–e19. [PubMed: 19965649]
36. Carlin LM, Stamatiades EG, Auffray C, Hanna RN, Glover L, Vizcay-Barrena G, Hedrick CC, Cook HT, Diebold S, Geissmann F. Nr4a1-dependent Ly6C(low) monocytes monitor endothelial cells and orchestrate their disposal. Cell. 2013; 153:362–375. [PubMed: 23582326]
37. Quintar A, McArdle S, Wolf D, Marki A, Ehinger E, Vassallo M, Miller J, Mikulski Z, Ley K, Buscher K. Endothelial Protective Monocyte Patrolling in Large Arteries Intensified by Western Diet and Atherosclerosis. Circ Res. 2017; 120:1789–1799. [PubMed: 28302649]
38. Greenberg ME, Li X-M, Gugiu BG, Gu X, Qin J, Salomon RG, Hazen SL. The Lipid Whisker Model of the Structure of Oxidized Cell Membranes. J Biol Chem. 2007; 283:2385–2396. [PubMed: 18045864]
39. Obergfell A, Eto K, Mocsai A, Buensuceso C, Moores SL, Brugge JS, Lowell CA, Shattil SJ. Coordinate interactions of Csk, Src, and Syk kinases with [alpha]IIb[beta]3 initiate integrin signaling to the cytoskeleton. J Cell Biol. 2002; 157:265–275. [PubMed: 11940607]

Highlights

- Nonclassical monocyte patrolling activity is increased in the vasculature during early atherogenesis.
- Patrolling speeds of nonclassical monocytes in Western-diet fed mice and in mice given OxLDL are reduced, suggesting a longer dwell time over a given area of endothelium.
- Patrolling activity of nonclassical monocytes was linked to oxidized LDL uptake by CD36.
- CD36 is required for nonclassical monocytes to effectively patrol and survey the endothelium during early atherogenesis.
- Human nonclassical monocytes also take up oxidized LDL.

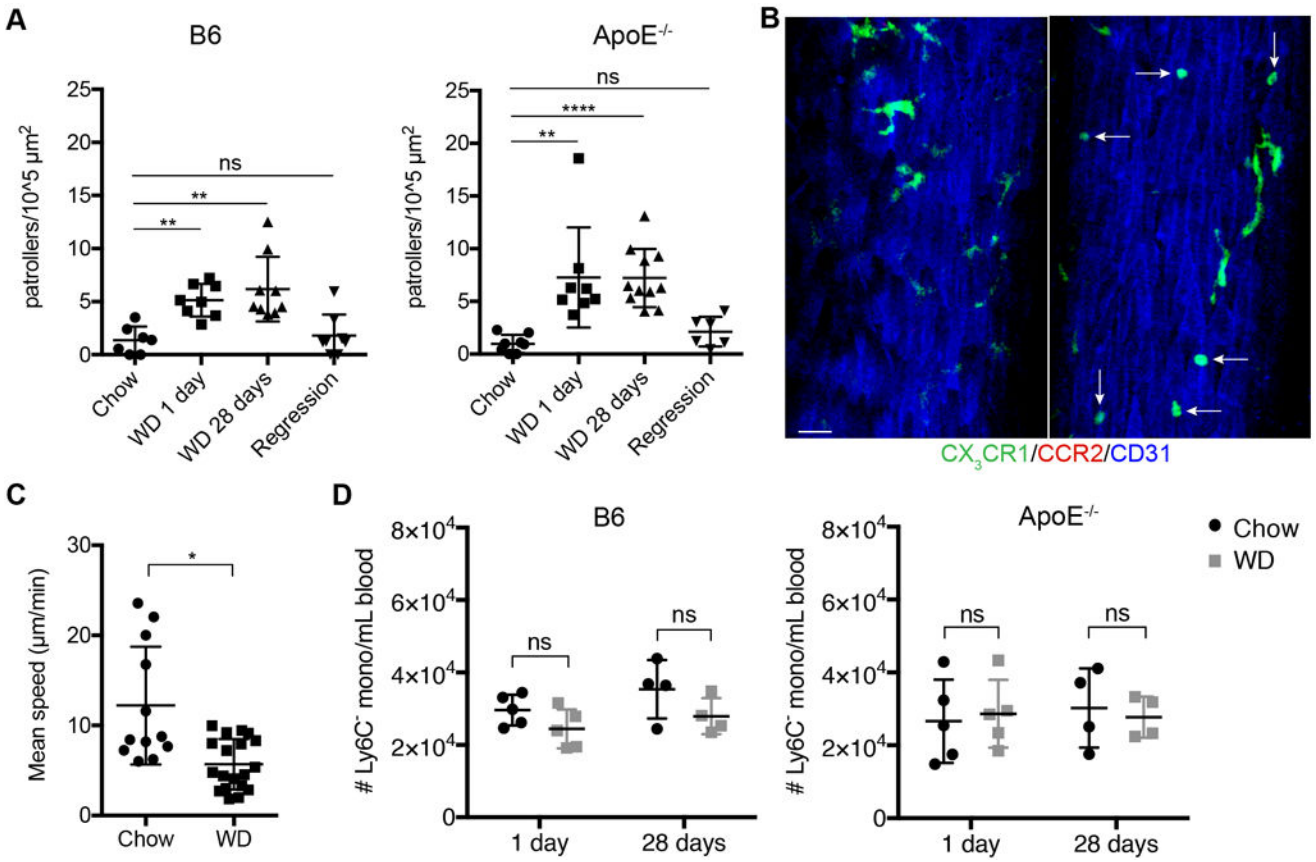

Figure 1.

Nonclassical monocyte patrolling activity increases in large peripheral blood vessels of mice fed a Western Diet. Age and sex-matched ApoE$^{-/-}$ and B6 mice were fed a WD for the times indicated and assessed for patrolling activity and monocyte frequency A, The number of CX_3CR1^{high} patrolling monocytes per surface area of blood vessel was determined for each recording (n=3 videos per mouse). Each point represents the total number of patrolling monocytes per total surface area of blood vessel for each mouse. n=6-11 mice per group. A Kruskal-Wallis test with Dunn's multiple comparison correction was used to analyze WD and Regression groups using Chow as the control group. B, Representative images of patrolling monocytes (highlighted by white arrows) in large blood vessels of ApoE$^{-/-}$ mice: CX_3CR1 (Ly6C$^-$ NCM), CCR2 (Ly6C$^+$ CM) and injected with anti-CD31 (endothelium). scale bars: 30 µM C, Patrolling speeds for NCM from ApoE$^{-/-}$ mice fed a Western diet (28 days) or chow. D, NCM numbers in blood were obtained by flow cytometry from chow and WD-fed mice. n=4-5 mice per group. Error bars represent mean ± SEM for all graphs. *P < 0.05, **P < 0.01, ****P < 0.0001, ns indicates not significant.

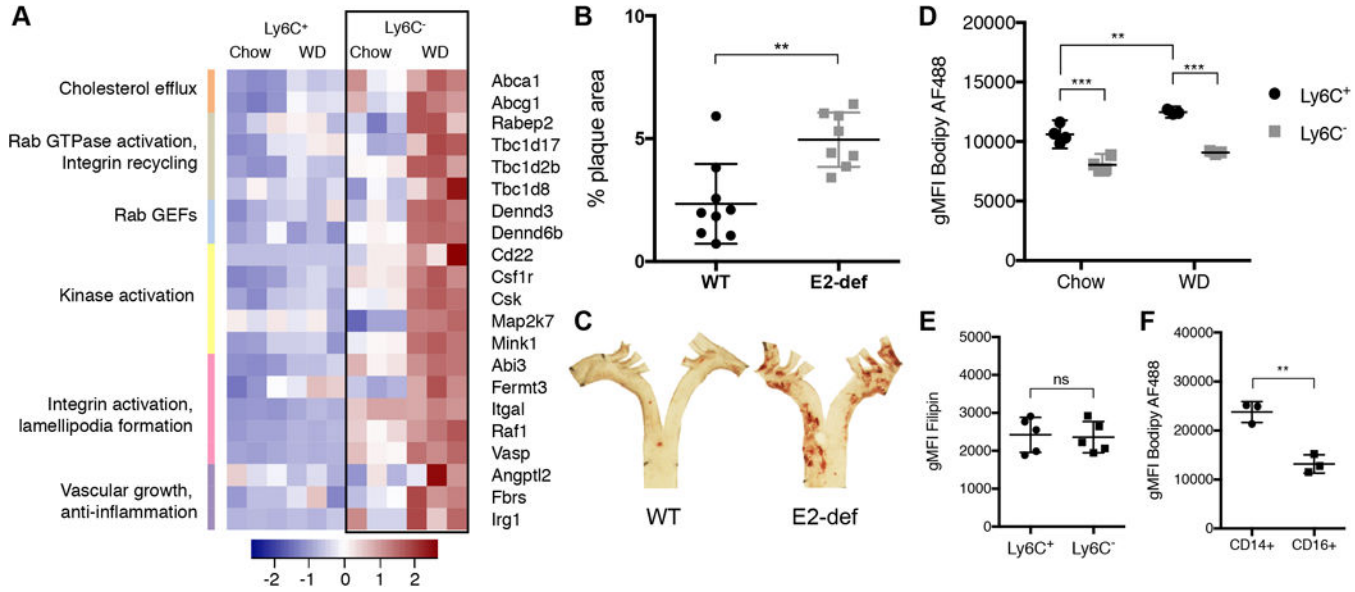

Figure 2.

Nonclassical monocytes from WD-fed mice are atheroprotective. A, Differential gene expression of RNA transcripts between monocyte subsets of WD or chow-fed mice. Ly6C^{+} and Ly6C^{-} monocyte subsets were sorted from chow or WD-fed mice. Genes of interest related to lipid metabolism, cell migration, and inflammation resolution that were uniquely upregulated in nonclassical monocytes from WD-fed mice are listed. n=30 mice (3 groups of 10 mice pooled). Statistical significance of upregulated genes was determined by False Discovery Rate (FDR) correction (Benjamini-Hochburg) with filtering of variance outliers by tagwise dispersion (>99.9%), P>0.001. B, Comparison of atherosclerotic plaque formation in B6 or E2 mice by en face Oil Red O (ORO) staining of aortas from mice fed a 15-week Western diet. Quantification of plaque area as a percentage of total aortic area. n=8-9 mice per group. C, Representative images of aortic root ORO staining. D, Bodipy staining of neutral lipids in blood monocyte subsets from chow and WD-fed mice by flow cytometry. n=4 mice per group. E, Filipin III staining of free cholesterol in blood monocyte subsets from chow-fed mice. n=5 mice. F, Bodipy staining of neutral lipids of blood monocyte subsets from healthy human donors by FACS. n=3 individuals. Error bars represent means ± SEM. **P < 0.01, ***P < 0.001, ns indicates not significant.

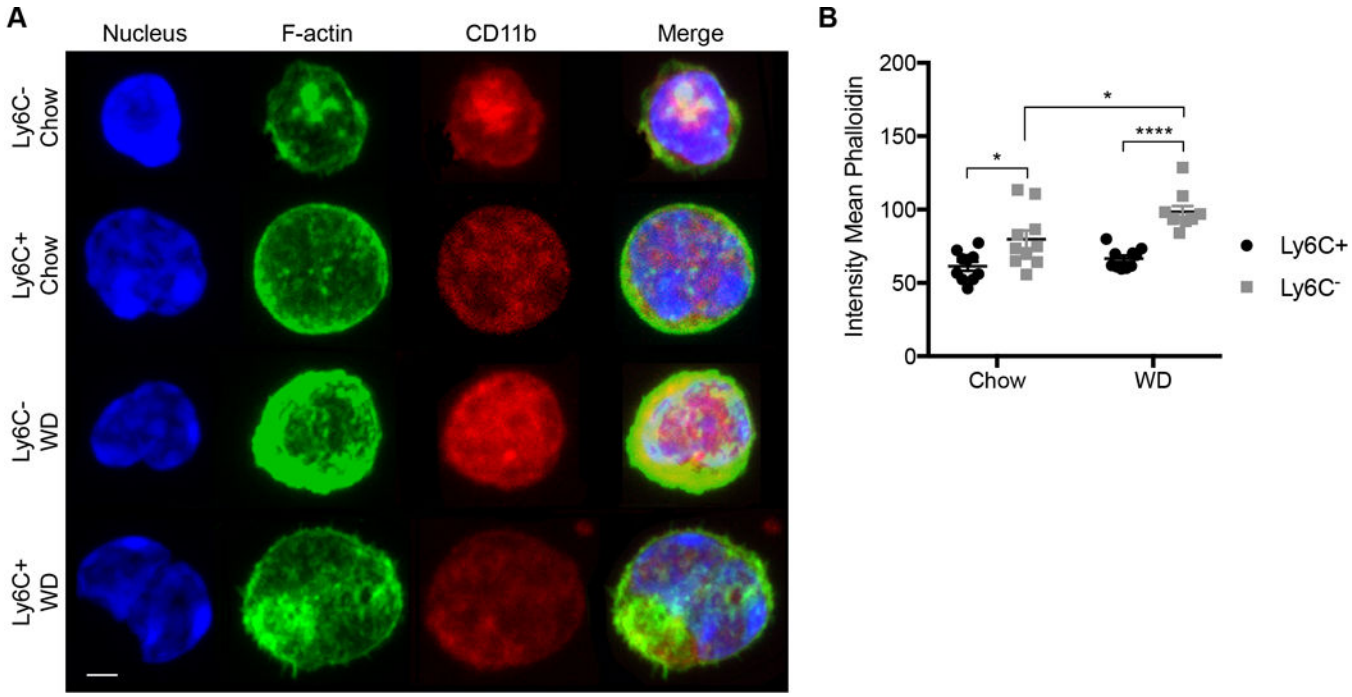

Figure 3.

Increased F-actin formation in nonclassical monocytes from mice fed a Western diet. A, Representative images of Ly6C^{+} (classical) and Ly6C^{-} (nonclassical) monocytes stained for F-actin formation using phalloidin-AF488 by confocal microscopy. scale bar = 2μM B, Mean intensity of F-actin staining (phalloidin-AF488) of monocyte subsets sorted from chow or WD-fed mice by confocal microscopy. n=10 cells per group. Error bars represent mean ± SEM for all graphs. *P < 0.05, ****P < 0.0001

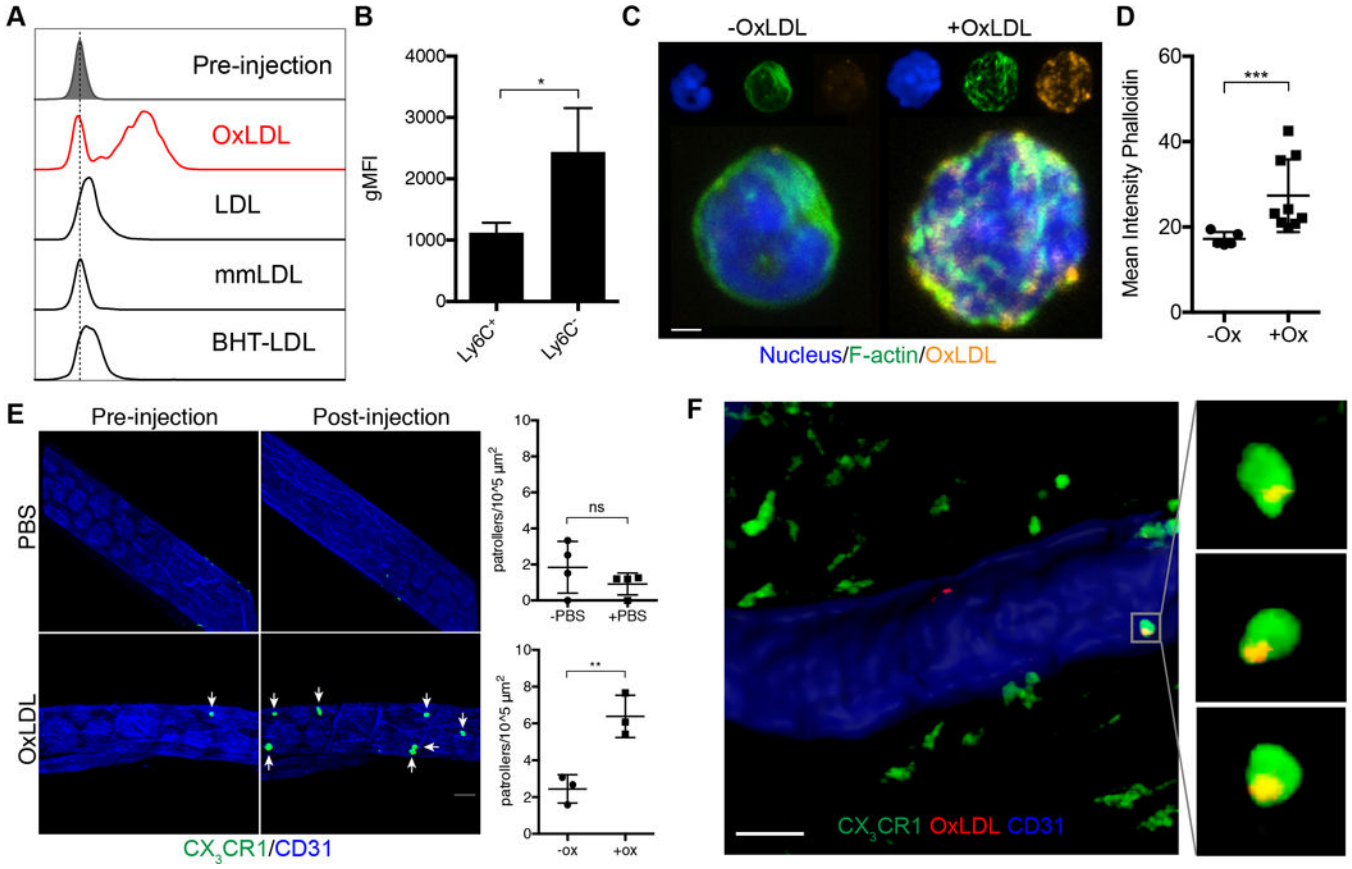

Figure 4.

OxLDL is preferentially taken up by nonclassical monocytes and induces NCM patrolling. A, Chow-fed ApoE$^{-/-}$ mice were injected with AF633-labeled OxLDL, LDL, mmLDL, or BHT-LDL. 15 minutes after injection, mice were analyzed for LDL uptake by flow cytometry (n=1 mouse per injection). Mice were anesthetized and bled prior to injection to obtain a baseline (Pre-injection). B, Comparison of AF633-labeled OxLDL uptake in Ly6C^{+} (CM) and Ly6C^{-} (NCM) blood monocyte subsets ex vivo by flow cytometry. n=3 mice. C, Representative images of F-actin staining in Ly6C^{-} monocytes incubated with or without OxLDL. Scale bar: 2 µM D, Quantification of F-actin mean fluorescent intensity of Ly6C^{-} monocytes with or without DiI-OxLDL. E, CX$_3$CR1$^{gfp/+}$ApoE$^{-/-}$ mice were imaged to obtain a baseline of patrolling frequency in a large blood vessel of a mouse leg (left column). PBS (100 µL) or OxLDL (100 µg) solutions were injected during imaging after obtaining a baseline. Timelapse images were obtained post-injection from the same pre-injected areas (right column). White arrows highlight patrolling NCM. Quantification of patrolling frequency before and after injection of PBS (upper graph) or OxLDL (lower graph) were graphed for each condition. n=3 independent experiments, one representative experiment shown. scale bar: 30 µM F, Representative figure of CX$_3$CR1$^{gfp/+}$ApoE$^{-/-}$ mice injected with DiI-OxLDL during imaging to observe OxLDL uptake by nonclassical monocytes while patrolling. n=2 independent experiments. scale bar: 30 µM. Error bars represent mean ± SEM for all graphs. *P < 0.05, **P < 0.01, ***P < 0.001.

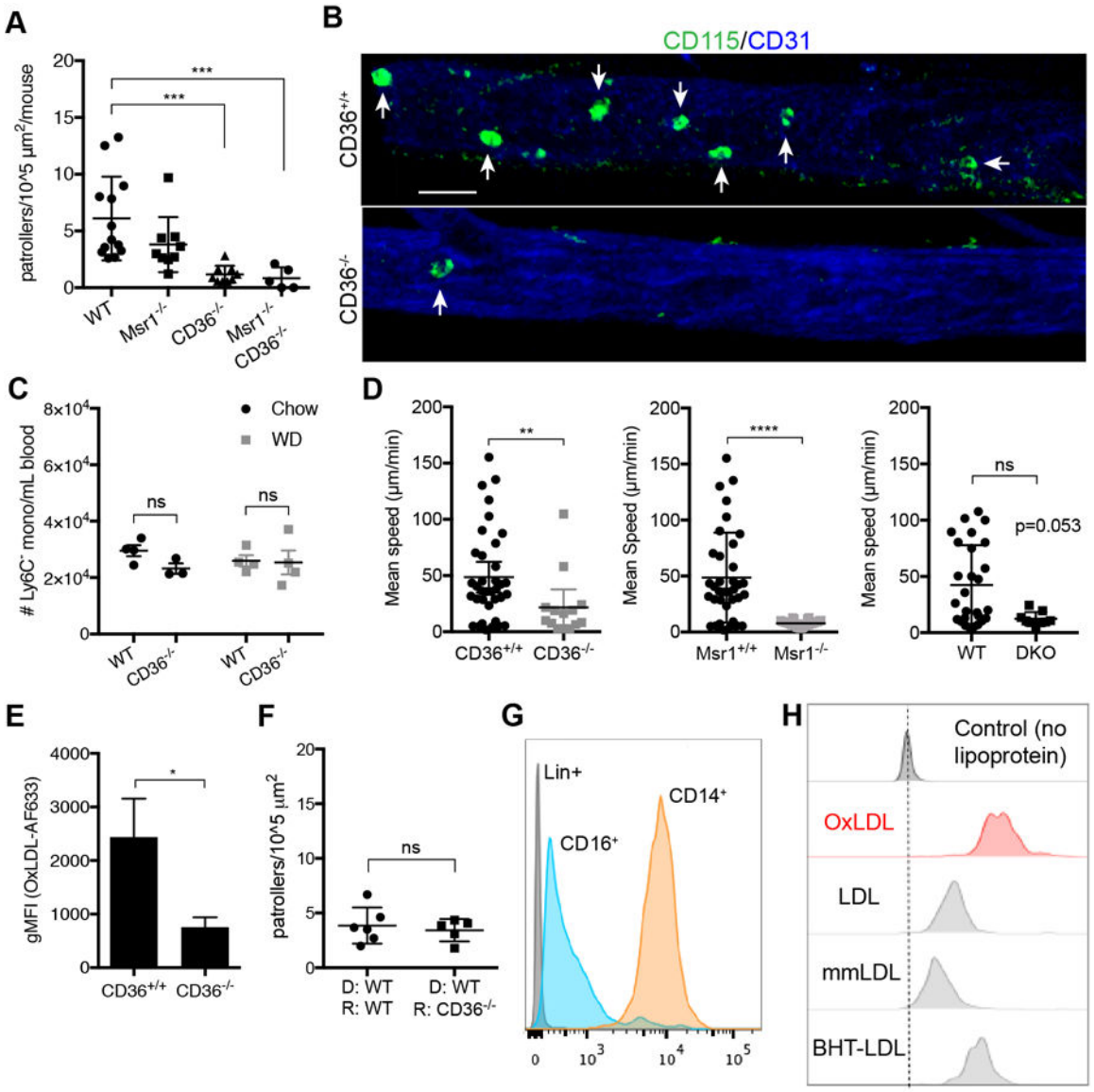

Figure 5.

CD36 is critical for nonclassical monocytes to patrol the vasculature in WD-fed mice. A, Mice were fed a WD for 28 days and imaged for patrolling activity. CD115 (shown in green) and FcγRIV antibodies were used to label nonclassical monocytes in vivo, blood vessels were labeled with CD31 antibody. Ratios of patrolling monocytes per surface area of each blood vessel recording (n=3 per mouse) were summed and reported per mouse. n=5-11 mice per group. B, Representative images of patrolling NCM (highlighted with white arrows) in mouse femoral vasculature obtained by intravital confocal microscopy. scale bar: 30 µM. C, Mean speeds of NCM for each imaging experiment shown in graph A. D, Frequencies of $Ly6C^{-}$ monocytes from retro-orbital bleeds of B6 or $CD36^{-/-}$ mice measured by FACS. n=3-4 mice per group. E, Blood monocytes were incubated ex vivo with AF633-labeled OxLDL and analyzed for uptake by flow cytometry. n=3 mice per group. F, WT $CX_3CR1^{gfp/+}$ bone marrow was transplanted into either WT recipients or $CD36^{-/-}$

recipients. Graph represents ratios of patrolling NCM per surface area of each blood vessel recording (n=3 per mouse) that were summed and reported per mouse. n=5-6 mice per group. G, Representative histogram of CD36 expression on $CD16^+$ monocytes from healthy human donors determined by flow cytometry. n=4 donors. H, Healthy human blood samples were incubated for 20 minutes at 37°C with AF633-labeled OxLDL, LDL, mmLDL, or BHT-LDL (and lineage antibodies) and measured by FACS for LDL uptake. Representative histogram of n=3 donors. Error bars represent mean ± SEM for all graphs. *P < 0.05, **P < 0.01, ***P < 0.001, ****P < 0.0001, ns indicates not significant

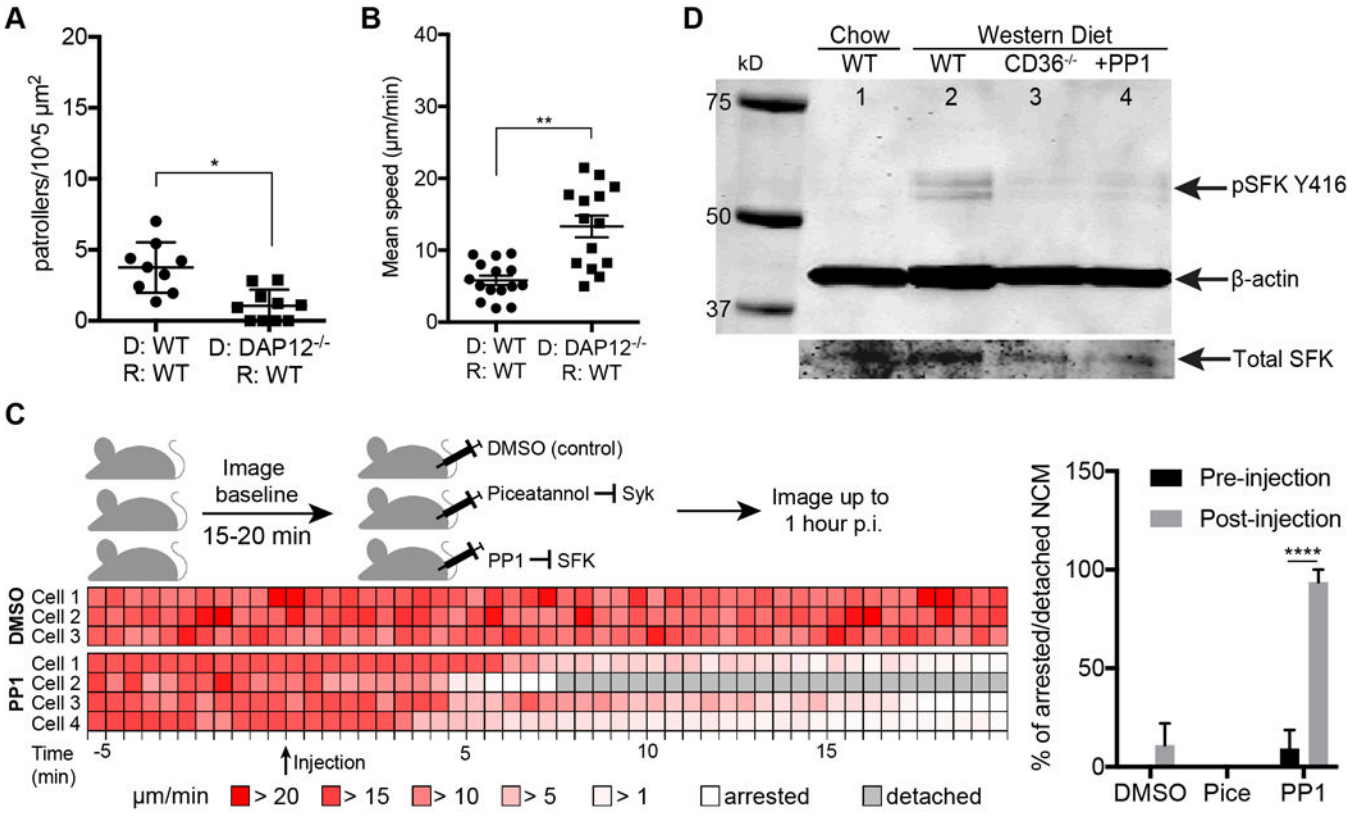

Figure 6.

Src family kinases mediates signaling downstream of CD36 through Dap12. A, DAP12$^{-/-}$ and B6 bone marrow chimeras were fed a WD and imaged by intravital microscopy for patrolling. Graph represents ratios of patrolling monocytes per surface area of each blood vessel recording (n=3 per mouse) that were summed and reported per mouse. n=9-10 mice per group. B, Mean speed of patrolling monocytes from mice fed a WD for 28 days. n=10 mice per group C, Representative western blot of phosphorylated Src family kinases (SFK) at Y416 with β-actin loading control. Blood monocytes were pooled and sorted from B6 mice fed chow (lane 1), WD (lane 2), CD36$^{-/-}$ WD-fed mice (lane 3), or monocytes from WD-fed mice incubated with PP1 (lane 4). Blots were stripped and reprobed for total protein for Src protein. D, $CX_3CR1^{gfp/+}CCR2^{rfp/+}ApoE^{-/-}$ mice on WD were imaged before (baseline) and after (post injection, p.i) injections of DMSO (vehicle, DMSO+PBS), Piceatannol (Syk inhibitor), or PP1 (SFK inhibitor). Each mouse was injected with 1 reagent and imaged intravitally to obtain patrolling speeds and behavior (arrest or detachment). Patrolling speed heat map represents each mouse injected with either DMSO or PP1 and plotted as each cell in the field of view in each mouse over time. Quantification of patrolling speeds were obtained with Imaris software and plotted in Excel. Bar graph shows what percent of NCM were arrested or detached after at 20 minutes post-injection listed on X-axis. n=2-3 mice per group. Error bars represent mean ± SEM for all graphs. *P < 0.05, **P < 0.01